PHYSICAL REVIEW B **79**, 241307(R) (2009)

Quantum analysis of shot noise suppression in a series of tunnel barriers

P. Marconcini, M. Macucci,* G. Iannaccone,* and B. Pellegrini*
Dipartimento di Ingegneria dell'Informazione, Università di Pisa, Via Caruso 16, I-56122 Pisa, Italy
(Received 10 February 2009; published 9 June 2009)

We report the results of an analysis, based on a straightforward quantum-mechanical model, of shot noise suppression in a structure containing cascaded tunneling barriers. Our results exhibit a behavior that is in sharp contrast with existing semiclassical models for this particular type of structure, which predict a limit of 1/3 for the Fano factor as the number of barriers is increased. The origin of this discrepancy is investigated and attributed to the presence of localization on the length scale of the mean free path, as a consequence of the strictly one-dimensional (1D) nature of disorder, which does not create mode mixing, while no localization appears in common semiclassical models. We expect localization to be indeed present in practical situations with prevalent 1D disorder, and the existing experimental evidence appears to be consistent with such a prediction.

DOI: 10.1103/PhysRevB.79.241307 PACS number(s): 73.23.Ad, 73.40.Gk, 72.70.+m

In the study of low-dimensional devices, suppression of shot noise with respect to the value predicted (for the case of a Poissonian noise process) by Schottky's theorem has represented one of the most active fields of investigation in the last two decades. Such a suppression phenomenon, described by means of the Fano factor, i.e., the ratio of the actual shot noise power spectral density to the full value $2q|I|$ (where q is the value of the elementary charge and I is the average value of the current flowing through the device), has been predicted and observed in many different mesoscopic structures and is the result of the presence of correlations between charge carriers, which reduce current fluctuations in the device. From the theoretical point of view, shot noise suppression has been investigated both with quantum-mechanical and with semiclassical approaches. Such activities have led to the discovery of "universal" values for the Fano factor in specific structures; in particular, for disordered conductors a universal suppression factor of 1/3 has been found both with random matrix theory[1,2] and with a semiclassical approach.[3] This result has received further confirmation from numerical simulations[4,5] and from experimental evidence.[6]

A remarkable addition to these results is a derivation by de Jong and Beenakker,[7,8] who demonstrated that a Fano factor of 1/3 is obtained, within a semiclassical model based on the Boltzmann-Langevin equation, also for a series of barriers. A formulation relying on an equivalent semiclassical circuit model (similar to that used in Ref. 9 for a series of chaotic cavities) leads to the same result.

However, the only existing experimental data,[10] obtained for a GaAs/AlGaAs superlattice, are not in agreement with these semiclassical conclusions: they exhibit a Fano factor that depends strongly on barrier transmission in the limit of vanishing applied electric field.

Prompted by this discrepancy, we have performed a quantum calculation of shot noise suppression for a structure consisting of cascaded barriers. While for a conductor with two-dimensional (2D) or three-dimensional (3D) disorder quantum simulations recover[4,5] exactly the same 1/3 suppression predicted by random matrix theory and by semiclassical models, this is not the case in the presence of one-dimensional (1D) disorder, i.e., of randomly spaced cascaded barriers, regardless of the dimensionality of the conductor. Our quantum calculations although performed for a model system do, instead, exhibit a behavior consistent with the experimental data.

In this Rapid Communication, we focus on the reasons for the discrepancies between the semiclassical and the quantum approaches and address the issue of what model best represents the situation of a practical experiment. The structure we have considered (a series of cascaded barriers, sketched in the inset of Fig. 1 and corresponding to that of Refs. 7 and 8) can be studied very straightforwardly from a numerical point of view. For each fixed value of the longitudinal coordinate x, the potential profile is constant for $0<y<W$ (y is the transverse coordinate, and W is the width of the structure: 8 μm in these calculations), while we assume a hard-wall confinement for $y=0$ and $y=W$. Thus, the orthonormal set of transverse modes is the same all over the structure, and the tunnel barriers do not introduce any mode mixing. Since the modes are uncoupled, the numerical analysis can be split into a set of one-dimensional problems, one for each considered mode. For the generic nth mode, the S matrices of an inter-barrier region of length L and of a tunnel barrier of height U and length l are

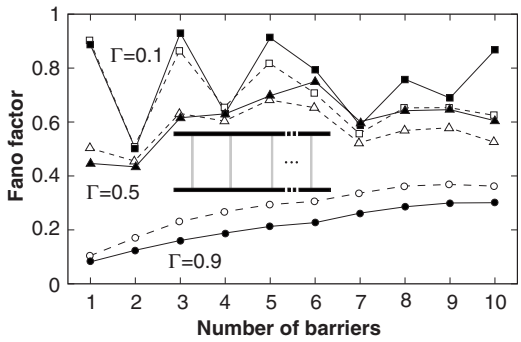

FIG. 1. Fano factor for a series of identical barriers, as a function of the number of barriers for the case of realistic barriers (solid lines), and for model barriers with a transparency independent of the longitudinal electron wave vector (dashed lines). Inset: sketch of the analyzed structure.

$$S_n = \begin{pmatrix} 0 & \tau_n \\ \tau_n & 0 \end{pmatrix}, \quad S_{B_n} = \begin{pmatrix} \rho_{B_n} & \tau_{B_n} \\ \tau_{B_n} & \rho_{B_n} \end{pmatrix}, \tag{1}$$

where (at the Fermi energy E_F)

$$\tau_n = \exp(ik_n L), \quad \rho_{B_n} = i\frac{k_{B_n}^2 - k_n^2}{2k_n k_{B_n}} \sin(k_{B_n} l)\tau_{B_n},$$

$$\tau_{B_n} = \left[\cos(k_{B_n} l) - i\frac{k_n^2 + k_{B_n}^2}{2k_n k_{B_n}} \sin(k_{B_n} l) \right]^{-1}, \tag{2}$$

with $k_n = \sqrt{k_F^2 - k_{T_n}^2}$, $k_{B_n} = \sqrt{k_F^2 - k_{T_n}^2 - k_U^2}$, $k_F = \sqrt{2mE_F}/\hbar$, $k_{T_n} = n\pi/W$, and $k_U = \sqrt{2mU}/\hbar$.

For each mode, the scattering matrices of adjacent slices are recursively composed to find the overall S matrix and in particular one of its elements, the transmission t_n of the nth mode through the device. The conductance and the shot noise power spectral density are then computed using the relations[11,12]

$$G = \frac{2q^2}{h}\sum_n T_n, \quad S_I = 4\frac{q^3}{h}|V|\sum_n T_n(1 - T_n), \tag{3}$$

where the sums are performed over all the N modes propagating in the interbarrier regions, $T_n = |t_n|^2$ and V is the externally applied voltage. Therefore the Fano factor γ can be computed as

$$\gamma = \frac{S_I}{2q|I|} = \frac{\sum_n T_n(1 - T_n)}{\sum_n T_n}. \tag{4}$$

Before computing the ratio, the values of the numerator and of the denominator are uniformly averaged over the range of energy qV, assuming it is much greater than $k\theta$ (where k is the Boltzmann constant and θ is the absolute temperature). In particular, our simulations have been performed using 500 values of energy in a range of 40 μeV around 9.03 meV.

In Fig. 1 we show, with solid lines, the values of the Fano factor obtained for an 8 μm wide structure made up of a series of identical barriers. In particular, the reported results are relative to 0.425 nm wide barriers, with heights equal to 0.8 (squares), 0.25 (triangles), and 0.07 eV (circles). These barriers (at the considered Fermi energy) have an average transparency $\Gamma = \Sigma_{n=1}^N |\tau_{B_n}|^2/N$ equal to about 0.1, 0.5, and 0.9, respectively. In these simulations the distance between adjacent barriers has been assumed to be $D + \delta$, where $D = 3$ μm, and (from left to right) $\delta = 0, 10, -6, 3, -3, -9, 5, -10, -2$ nm.

We see that, as expected, for all transparencies the Fano factor for a single barrier is about $1-\Gamma$ (not exactly $1-\Gamma$ because different modes experience different transparencies and Γ is only an average value). For two barriers our results are still in agreement with the semiclassical model of Ref. 7 and, specifically, with the results of its Eq. (17). For more than two barriers we notice a sharp divergence from the semiclassical prediction and that no asymptotic 1/3 value is reached. Indeed, our results show some dependence on the interbarrier spacings, but the overall behavior is already captured by the plots of Fig. 1. A marked difference is observed only in the case of equidistant barriers, in which strong resonances between the different interbarrier regions play a major role, a case that we do not address in detail in this Rapid Communication.

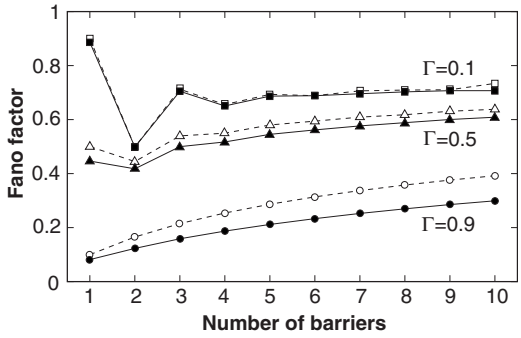

FIG. 2. Same quantities as in Fig. 1 but averaged over 50 sets of interbarrier distances.

We have also repeated our simulations making the same simplification adopted (for analytical convenience) in Ref. 7, i.e., assuming a barrier transparency independent of the orthogonal wave vector of the impinging particle. In detail, we have replaced the previously indicated scattering matrix for a barrier with that of an artificial barrier in which $\rho_{B_n} = -i\sqrt{1-\Gamma}$ and $\tau_{B_n} = \sqrt{\Gamma}$, with Γ being the wave-vector-independent transparency. No significant variation is observed in the Fano factor when such a change is included in our calculation (see dashed lines in Fig. 1).

In order to remove the dependence of our results on the actual choice of the set of lengths of the interbarrier regions, we have performed an average over several sets.[13] It has been shown that a similar approach is able to reproduce many effects of dephasing on transport.[14] The results obtained by averaging over energy values and over 50 different sets of interbarrier distances are shown in Fig. 2 as a function of the number of cascaded barriers for the same transparency values as in Fig. 1, assuming either a realistic barrier model (solid lines) or a wave-vector-independent transparency (dashed lines). Also in this case there is no clear convergence to a common value of 1/3.

If we consider a situation with cascaded identical barriers characterized by transparencies that are independent of the wave vector and average over random phases, all propagating modes give the same contribution to the noise behavior because the different values of the longitudinal wave vectors are made irrelevant. Therefore it becomes possible to perform an analytical calculation of the Fano factor by considering a single mode and integrating over the phase of τ_n between 0 and 2π for each interbarrier region. The analytical treatment can be carried out for the cases of two and three cascaded barriers (with transparency Γ), for which we obtain, respectively,

$$\gamma_2 = \frac{2(1-\Gamma)}{(2-\Gamma)^2} \quad \text{and} \quad \gamma_3 = \frac{3(4 - 8\Gamma + 5\Gamma^2 - \Gamma^3)}{16 - 24\Gamma + 9\Gamma^2}, \tag{5}$$

which are in agreement with the numerical results represented with dashed lines in Fig. 2. Coherently with our pre-

vious discussion, the result for two barriers coincides with that from the semiclassical model of Ref. 7, while that for three barriers does not. This is consistent with the conclusions by Förster *et al.*,[15] who show that only in the case of a single probe (in our structure a probe should be included between each pair of barriers), current fluctuation statistics do not depend on the nature (phase averaging, elastic dephasing, or inelastic) of the probe itself.

The key difference between the semiclassical and the quantum model consists in the fact that a semiclassical model (unless very peculiar assumptions are made[16]) lacks localization as a result of complete incoherence, while a quantum model does exhibit strong localization.[17] In particular the one-dimensional nature of the disorder represented by the randomly placed barriers makes the system effectively one-dimensional regardless of its actual dimensionality. In this case no mode mixing is introduced, and therefore the localization length is of the order of the mean free path; localization occurs beyond this length. Instead, in the case of two- or three-dimensional disorder, as in Refs. 4 and 5, strong mode mixing makes the localization length approximately equal to the mean free path times the number of propagating modes.[18]

In addition, in the absence of mode mixing, it is not possible to consider the interbarrier regions as quasireservoirs, characterized by a well-defined occupancy, that depends only on the energy. This assumption is at the basis of the calculations of Refs. 7–9, as well as of the semiclassical Monte Carlo numerical simulation by Liu *et al.*[19]

Instead, in the absence of mode mixing, only a mode-dependent occupancy can be defined; we have computed it for the same structure as in Fig. 1, in which all possible electron states can be divided into two sets: those injected from the left lead and those injected from the right lead. Therefore, if we define as ψ_{n_L} and ψ_{n_R} the electron wave functions in the generic interbarrier region Ω resulting from an injection of the nth mode (with unit probability current) from the left or right lead (respectively), the occupancy f_{n_Ω} in the region Ω for the nth mode can be expressed as the ratio of the partial density of states related to injection from the left to the total density of states for that mode:[20]

$$f_{n_\Omega} = \frac{\int_\Omega |\psi_{n_L}|^2 dxdy}{\int_\Omega |\psi_{n_L}|^2 dxdy + \int_\Omega |\psi_{n_R}|^2 dxdy}. \quad (6)$$

Results for the occupancy in the five interbarrier regions of a series of six unequally spaced barriers with an average transparency $\Gamma=0.1$ are reported in Fig. 3 for a selection of eight of the 320 propagating modes. It is apparent that these occupancies assume quite different values, with a strong dispersion that clearly appears in the inset, where we present the distribution of the occupancy in the region between the third barrier and the fourth barrier. Therefore the assumption of quasireservoir behavior of the interbarrier regions is definitely not valid in this case. An exception is confirmed for the case of just two barriers (thus with a single interbarrier region), in which the occupancies are all equal and corresponding to the value predicted by semiclassical models.

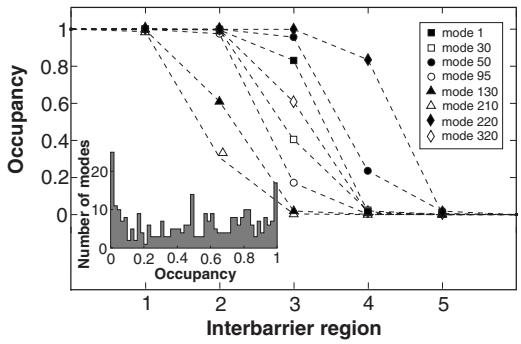

FIG. 3. Values of the occupancy for eight modes in the five interbarrier regions of a series of six unequally spaced tunnel barriers with $\Gamma=0.1$. Inset: distribution of the occupancy for the propagating modes in the third interbarrier region.

In the presence of mode mixing, instead, the localization length L_l is approximately equal, as already mentioned, to the product of the elastic mean free path L_0 by the number of propagating modes N; therefore there can be a range of device length L_d values in which the condition for diffusive transport ($L_0 \ll L_d \ll NL_0$) is satisfied, and thus the Fano factor can possibly reach the value 1/3 (as in the case of 2D or 3D disorder).

An adjustable amount of mode mixing can be introduced by applying a magnetic field orthogonal to the plane containing the device. We have computed the Fano factor for a 1 μm wide structure with a series of ten unevenly spaced barriers, with average interbarrier distance 500 nm. The results, obtained averaging over a number of interbarrier distance sets (40 for $\Gamma=0.1$, 30 for $\Gamma=0.25$, 20 for $\Gamma=0.5$, and 10 for $\Gamma=0.75$ and $\Gamma=0.9$) are reported in the inset of Fig. 4 for different choices of the barrier transparency Γ. In detail, the barriers are 66 meV high, with a thickness of 4, 2.6, 1.56, 0.85, and 0.4 nm for the five considered transparencies; the Fermi energy is 9.03 meV. We observe that, after a quick drop, as the magnetic field increases the Fano factor settles around values that depend on barrier transparency. In the main panel of Fig. 4 we report the Fano factor for a constant

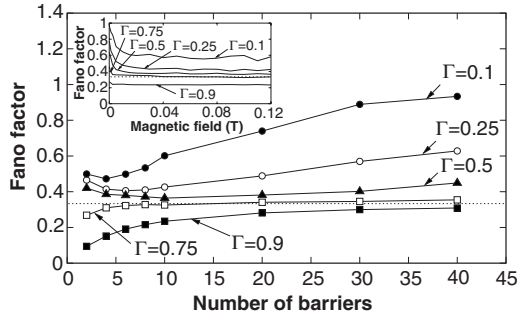

FIG. 4. Values of the Fano factor obtained for a series of identical barriers in a 1 μm wide structure with an orthogonal magnetic field $B=0.1$ T, represented as a function of the number of barriers. In the inset: Fano factor for a series of 10 identical barriers, as a function of magnetic field. The dotted lines indicate the diffusive limit of 1/3.

magnetic field of 0.1 T as a function of the number of barriers. We notice that for large values of the transparency and thus large values of the mean free path, a diffusive transport regime (with a Fano factor of 1/3) is achieved only for a length much larger than the mean free path. On the other hand, for low barrier transparencies and therefore reduced mean free path, localization effects appear before reaching the diffusive limit. To prevent this, we should significantly increase the number of propagating modes and thus the localization length.

The issue is then whether in a practical system containing cascaded barriers large enough mode mixing takes place. Besides magnetic field, possible mechanisms leading to mode mixing are scattering with irregularities in the potential (2D or 3D disorder) or phonon scattering. Scattering due to a disordered potential landscape can well lead to full mode mixing, but in such a case the Fano factor of 1/3 characteristic of diffusive transport is achieved anyway, independent of the presence of the barriers and cannot therefore be specifically attributed to their action. As far as phonon scattering is concerned, it can in principle introduce mode mixing, but in the presence of strong phonon interaction the transport regime would not be the one we are interested in, and thermal noise would prevail.

A Fano factor of 1/3 might in principle also be recovered, irrespective of the degree of mode mixing, in the presence of a hypothetical elastic mechanism capable of suppressing phase coherence completely.

The relatively large values of the phase coherence length that can be achieved in modern materials at low temperature and the low-field results for the Fano factor presented in Ref. 10 lead us to the conclusion that a superlattice or a series of electrostatically defined barriers in a channel containing a high-mobility two-dimensional electron gas are more likely to exhibit localization and a Fano factor as predicted by our model rather than a diffusive behavior. Numerical approaches along the lines we have presented could be instrumental in designing further experimental tests, which should be performed on structures with unevenly spaced barriers.

We are indebted to C. W. J. Beenakker for useful discussion.

*Also at CNR-IEIIT (Pisa), Via Caruso 16, I-56122 Pisa, Italy.

[1] C. W. J. Beenakker and M. Büttiker, Phys. Rev. B **46**, 1889 (1992).
[2] R. A. Jalabert, J.-L. Pichard, and C. W. J. Beenakker, Europhys. Lett. **27**, 255 (1994).
[3] K. E. Nagaev, Phys. Lett. A **169**, 103 (1992).
[4] A. Kolek, A. W. Stadler, and G. Haldaś, Phys. Rev. B **64**, 075202 (2001).
[5] M. Macucci, G. Iannaccone, G. Basso, and B. Pellegrini, Phys. Rev. B **67**, 115339 (2003).
[6] M. Henny, S. Oberholzer, C. Strunk, and C. Schönenberger, Phys. Rev. B **59**, 2871 (1999).
[7] M. J. M. de Jong and C. W. J. Beenakker, Phys. Rev. B **51**, 16867 (1995).
[8] M. J. M. de Jong and C. W. J. Beenakker, Physica A **230**, 219 (1996).
[9] M. Macucci, P. Marconcini, and G. Iannaccone, Int. J. Circuit Theory Appl. **35**, 295 (2007).
[10] W. Song, A. K. M. Newaz, J. K. Son, and E. E. Mendez, Phys. Rev. Lett. **96**, 126803 (2006).
[11] G. B. Lesovik, Pis'ma Zh. Eksp. Teor. Fiz. **49**, 513 (1989); JETP Lett. **49**, 592 (1989).
[12] M. Büttiker, Phys. Rev. Lett. **65**, 2901 (1990).
[13] R. Landauer, Philos. Mag. **21**, 863 (1970).
[14] M. G. Pala and G. Iannaccone, Phys. Rev. B **69**, 235304 (2004); Phys. Rev. Lett. **93**, 256803 (2004).
[15] H. Förster, P. Samuelsson, S. Pilgram, and M. Büttiker, Phys. Rev. B **75**, 035340 (2007).
[16] H. Schanz and U. Smilansky, Phys. Rev. Lett. **84**, 1427 (2000).
[17] P. W. Anderson, D. J. Thouless, E. Abrahams, and D. S. Fisher, Phys. Rev. B **22**, 3519 (1980).
[18] H. Tamura and T. Ando, Phys. Rev. B **44**, 1792 (1991).
[19] R. Liu, P. Eastman, and Y. Yamamoto, Solid State Commun. **102**, 785 (1997).
[20] G. Iannaccone, Phys. Rev. B **51**, 4727 (1995).